Dishevelled phosphorylation, subcellular localization and multimerization regulate its role in early embryogenesis

Ute Rothbächer[1,2,3], Micheline N.Laurent[4], Matthew A.Deardorff[5], Peter S.Klein[5], Ken W.Y.Cho[4] and Scott E.Fraser[1,3]

[1]Division of Biology and Beckman Institute, California Institute of Technology, Pasadena, CA 91125, [4]Department of Developmental and Cell Biology, University of California at Irvine, Irvine, CA 92697 and [5]Cell and Molecular Biology, Howard Hughes Medical Institute and Department of Medicine, University of Pennsylvania School of Medicine, Philadelphia, PA, USA

[2]Present address: Laboratoire de Genetique et Physiologie du Developpement, IBDM, Campus de Luminy, Marseille, France

[3]Corresponding authors
e-mail: rothbach@lgpd.univ-mrs.fr or sefraser@caltech.edu

K.W.Y.Cho and S.E.Fraser contributed equally to this work

Dishevelled (Dsh) induces a secondary axis and can translocate to the membrane when activated by Frizzleds; however, dominant-negative approaches have not supported a role for Dsh in primary axis formation. We demonstrate that the Dsh protein is post-translationally modified at the dorsal side of the embryo: timing and position of this regulation suggests a role of Dsh in dorsal–ventral patterning in *Xenopus*. To create functional links between these properties of Dsh we analyzed the influence of endogenous Frizzleds and the Dsh domain dependency for these characteristics. *Xenopus* Frizzleds phosphorylate and translocate Xdsh to the membrane irrespective of their differential ectopic axes inducing abilities, showing that translocation is insufficient for axis induction. Dsh deletion analysis revealed that axis inducing abilities did not segregate with Xdsh membrane association. The DIX region and a short stretch at the N-terminus of the DEP domain are necessary for axis induction while the DEP region is required for Dsh membrane association and its phosphorylation. In addition, Dsh forms homomeric complexes in embryos suggesting that multimerization is important for its proper function.
Keywords: axis formation/DEP/Dishevelled/Frizzled/Wnt signaling

Introduction

The differential activation of members of the Wnt signaling pathway (β-catenin in particular) is the earliest known molecular manifestation of dorsal–ventral patterning in amphibians (for a review see Moon and Kimelman, 1998). How this pathway is activated regionally in the embryo remains one of the key questions in developmental biology. Recently, understanding of the Wnt pathway has progressed significantly by studies in various model systems. Wnt molecules belong to an increasingly large family of growth factors (19 members to date) and are thought to bind to the Frizzled family of seven-transmembrane domain molecules (Bhanot *et al.*, 1996). In many systems, binding of Wnts to these putative receptors may induce the activation of intracellular Dishevelled (Dsh), which in turn regulates the activity of the serine-threonine kinase GSK-3/Zw-3/Sgg (for a review see Cadigan and Nusse, 1997). In the absence of signal, GSK-3 phosphorylates β-catenin/Armadillo, resulting in its high turnover rate; however, activation of Dsh inhibits GSK-3 and leads to the stabilization and accumulation of β-catenin in the cytoplasm, promoting its interaction with members of the Tcf/Lef-1/pangolin family of DNA-binding molecules to influence target gene expression.

In *Xenopus*, the Wnt pathway is crucial for proper dorso-ventral axis specification (for reviews see Miller and Moon, 1996; Heasman, 1997; Moon and Kimelman, 1998). First, depletion of maternal β-catenin prevents the formation of the embryonic axis. Secondly, ectopic expression of Xwnt8, Xdsh, β-catenin or dominant-negative GSK-3 leads to secondary axis formation. Thirdly, Wnt signaling directly affects the transcription machinery in the Spemann's organizer (Rothbächer *et al.*, 1995; Watabe *et al.*, 1995), and organizer-specific homeobox genes *Xsiamois* and *Xtwin* are direct transcriptional targets of the β-catenin–Tcf complex (Brannon *et al.*, 1997; Laurent *et al.*, 1997). While these pieces of evidence demonstrate the importance of the Wnt pathway, it is still not clear how this pathway is first activated in embryos. One possibility is that an endogenous maternal Wnt regulates this process. However, thus far, no Wnt molecule has been demonstrated to display a spatio-temporal pattern of expression compatible with a role during axis formation. An alternative model favors activation of members of the pathway downstream of Dsh. In support of this hypothesis is the observation that β-catenin becomes activated at the site of the future dorsal organizer, whereas dominant-negative versions of Wnt-8, Frizzled (or wild-type FRP/FrzB) and Xdsh have been reported to fail at blocking the endogenous axis formation of embryos. However, such negative results must be interpreted cautiously, as dominant-negative approaches can fail to abolish interactions of endogenous proteins. For instance, if endogenous molecules are already pre-engaged in stable complexes, the complex might be unaltered by the later expression of the dominant-negative protein (Wittbrodt and Rosa, 1994). Thus, the involvement of the Wnt pathway upstream of GSK-3 in the specification of the endogenous axis must still be considered an open question.

The role of Dsh is not well understood. In addition to mediating the classical Wnt pathway, Dsh affects cell polarity (Theisen *et al.*, 1994; Heslip *et al.*, 1997) and interacts with Notch signaling (Ruel *et al.*, 1993; Couso and Martinez Arias, 1994; Axelrod *et al.*, 1996). The

presence of multiple domains in Dsh suggests that it may interact with different signaling pathways via different domains. Several structural motifs are conserved in Dsh of various species, ranging from *Caenorhabditis elegans* to humans (our observations, Figure 3; and Sussman *et al*., 1994; Sokol *et al*., 1995; Klingensmith *et al*., 1996; Tsang *et al*., 1996; Yang *et al*., 1996; Semenov and Snyder, 1997). The N-terminal DIX domain (DIX named after Dishevelled and axin) can interact physically with and has homologies to the C-terminal region of axin, a negative regulator of Wnt signaling (Zeng *et al*., 1997; Hamada *et al*., 1999; Kishida *et al*., 1999, Li *et al*., 1999a; Smalley *et al*., 1999). The medial PDZ domain of Dsh represents a globular protein–protein interaction domain contained in many adaptor molecules found in cellular junctional complexes. PDZ domains bind C-terminal ends of membrane receptors and/or interact with other PDZ domains (Kennedy, 1995; Ponting *et al*., 1997). Finally, the C-terminal DEP domain (named after Dishevelled, Egl-10 and plekstrin) is found in several molecules that regulate G-protein functions (Ponting and Bork, 1996). Although the high conservation of the Dsh domains is likely to reflect their conserved properties in embryogenesis (Rothbächer *et al*., 1995), much of their functional significance has yet to be determined. Only recently, the DEP region of *Drosophila* Dsh has been shown to play a role in tissue polarity in *Drosophila* (Axelrod *et al*., 1998; Boutros *et al*., 1998). Thus, understanding how Dsh mediates differential cellular responses in a given biological context is central to elucidating how Wnt signaling pathways can be activated in the embryo.

In order to elucidate the function of Dsh, we have analyzed various properties of the Dsh protein in early *Xenopus* embryogenesis. We show that Dsh is regulated post-translationally by phosphorylation at the right time and place to be involved in early dorso-ventral axis specification of the embryo. *Xenopus* Frizzleds present in early embryos all influence the intracellular localization of Dsh, suggesting their endogenous interaction with Dsh. To understand the mechanism of action of Dsh and to assign roles to the conserved domains of Dsh in *Xenopus*, we generated various deletion constructs within the conserved regions of Dsh and tested their ability to accumulate at the membrane, to induce ectopic axes and to be phosphorylated in *Xenopus* embryos. Additionally, we find that Xdsh forms homomeric complexes irrespective of the presence or absence of Frizzled, raising the possibility that dimerization is important for the proper functions of Dsh. If so, dominant-negative approaches may have limited utility for disrupting endogenous Dsh functions. We propose a model where Dsh is a homomeric, multi-modular protein that mediates different functions by distinct domains at different subcellular locations and may participate in setting up dorsal–ventral differences in the embryo.

Results

### *Dynamic post-translational modification of endogenous Xdsh*

Xenopus Dsh (*Xdsh*) mRNA is expressed abundantly in early embryos (Rothbächer *et al*., 1995; Sokol *et al*., 1995) and Xdsh protein is present throughout early *Xenopus* development (Figure 1B). Xdsh protein migrates as two

major bands, as revealed by analysis using crude extracts of embryos isolated from various stages of development (Figure 1B and C). Likewise, immunoprecipitations of ectopically expressed epitope-tagged Xdsh (Xdsh-HA) identified two similarly migrating bands (Figure 1A and D). As previous work suggested that *Drosophila* and mouse Dishevelled are phosphorylated (Yanagawa *et al*., 1995; Semenov and Snyder, 1997), we examined this possibility in *Xenopus*. Immunoprecipitated Xdsh-HA treated with acid phosphatase migrates as a single band of 80 kDa (Figure 1A), suggesting that the higher molecular weight band represents mobility shifted, phosphorylated Xdsh and the lower molecular weight band is non- or poorly phosphorylated Xdsh.

The phosphorylation profile of Xdsh varies at developmental stages (Figure 1B). Initially, Xdsh isolated from oocytes (not shown) and from early (post-fertilized) embryos migrates as a single band. During early cleavage stages, the mobility-shifted (phosphorylated) form appears as early as the 16-cell stage, continues to accumulate until blastula stage and then decreases slightly during gastrulation.

The timing of the developmental changes in Xdsh phosphorylation is suggestive of its early role in development. Shortly after fertilization, cytoplasmic rearrangements occur to translocate vegetal components to the dorsal side of the embryo. As development proceeds, dorsally located cells show accumulation of β-catenin (Schneider *et al*., 1996; Larabell *et al.*, 1997; Rowning *et al*., 1997). To determine whether the phosphorylation of Xdsh correlates with the onset of dorsalizing events, we analyzed the degree of Xdsh phosphorylation in dorsal (D) and ventral (V) explants. At the 64- to 128-cell stage, when phosphorylation reaches a peak, phosphorylated Xdsh is detected more abundantly in the dorsal region (Figure 1B, compare D with V). Densitometric quantitation of panels D and V shown in Figure 1B shows a 1.35-fold difference of lower migrating, underphosphorylated bands and a 3.85-fold difference in higher migrating, phosphorylated bands. Thus, a 2.8-fold higher level of phosphorylation is detected in dorsal explants even after normalizing the amount of underphosphorylated Xdsh protein in dorsal and ventral samples (for details, see Materials and methods). β-catenin levels (not shown) were 2.2-fold higher in dorsal samples. The experiment was performed twice, with similar results. No significant differences in Xdsh phosphorylation were detected between dorsal and ventral halves at late blastula and early gastrula stages (data not shown). Thus, phosphorylation of Xdsh parallels the activation of dorsal determinants in time and place. Together with β-catenin nuclear accumulation, the differential phosphorylation of Xdsh is the earliest molecular manifestation of events that break the radial symmetry in the embryo.

The above results may suggest that phosphorylation of Xdsh is involved in axis formation. Two classes of findings indicate that the role of Xdsh phosphorylation should be examined carefully. First, doses of Xdsh mRNA required to induce ectopic axes do not correlate well with the levels of Xdsh phosphorylation (Figure 1C). The extent of the induced ectopic axis is concentration dependent, i.e. increasing concentrations of injected RNA induce progressively stronger secondary axis (data not shown, see
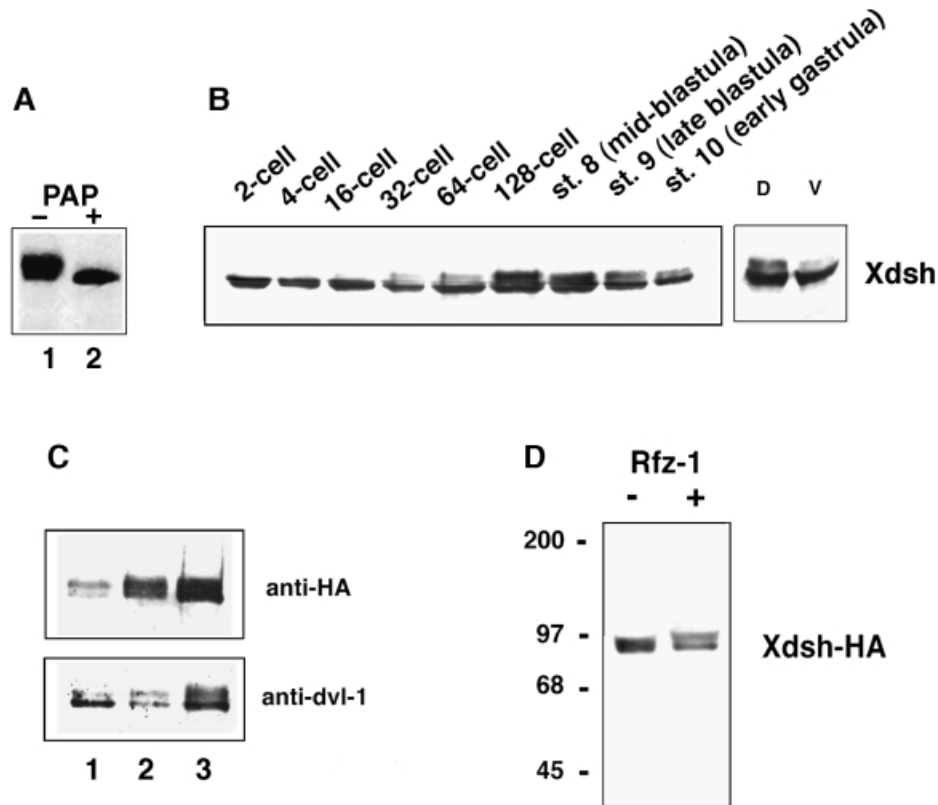
Fig. 1. Xdsh is phosphorylated differentially during development. (**A**) Slower migrating forms of Xdsh are caused by phosphorylation. Phosphatase treatment of Xdsh-HA immunoprecipitates from blastula embryos injected with 1 ng of mRNA at the 4-cell stage. Precipitates were incubated with (+) or without (–) potato acid phosphatase (PAP). The blot is stained with anti-HA antibody. (**B**) Developmentally regulated phosphorylation of endogenous Xdsh in post-fertilization stages. Left panel: endogenous Xdsh phosphorylation in embryonic extracts at various early stages of development. Right panel: extracts of dorsal (D) and ventral (V) halves at the 64- to 128-cell stage, stained with anti-*Drosophila* Ddsh antiserum. An equivalent of two embryos is shown per lane. At the 64- to 128-cell stage, Xdsh phosphorylation is significantly higher in the dorsal half of embryos. (**C**) Increased phosphorylation following Xdsh overexpression. Upon injection of 0.05 ng (1), 0.5 ng (2) or 1 ng (3) of Xdsh-HA mRNA in 4-cell embryos and collection of extracts at blastula stages, a higher ratio of phosphorylated versus non-phosphorylated forms is observed in ectopic Xdsh (upper panel, anti-HA stain) when compared with endogenous Xdsh (lower panel, anti-Dvl-1 stain) in the same samples. Higher amounts of ectopic Xdsh only slightly increase the phosphorylation of endogenous Xdsh (compare lanes 1 and 3). (**D**) Xdsh is hyperphosphorylated upon rat *frizzled-1* co-expression. Co-injection of 0.5 ng of Xdsh-HA and 1 ng of rat Frizzled-1 (Rfz-1) mRNA (+) leads to a shift of slower migrating, phosphorylated bands when compared with injection of Xdsh-HA mRNA only (–). Blots of anti-HA precipitations were stained with anti-HA antibody. The two Xdsh bands are not well separated due to a shorter electrophoresis run in (D).

also Figure 6 and Materials and methods). In contrast, phosphorylation levels are not proportional to the amount of injected RNA, and even low concentrations of ectopic Xdsh are highly phosphorylated (Figure 1C, compare lanes 1 and 3). It is possible, however, that phosphorylated Xdsh accumulates at high ectopic Xdsh concentrations to threshold levels necessary for ectopic axis induction. Secondly, we find that overexpression of rat *frizzled-1* alone does not induce secondary axis formation in *Xenopus* (data not shown) but can induce the translocation of ectopic Xdsh to the membrane (Yang-Snyder *et al.*, 1996) and causes a marked increase in mobility-shifted, hyperphosphorylated Dsh (compared with injection of Xdsh alone; Figure 1D). Taken together, these findings indicate that Dsh phosphorylation may be correlated better with its translocation to the membrane; variations in other components, such as binding of Xdsh-interacting molecules and/or activity changes in Xdsh, might then result in the axis-inducing dose–response curve.

Membrane association and hyperphosphorylation of Xdsh by Xenopus Frizzleds are independent of their axis-inducing abilities

Our results suggest that Xdsh phosphorylation in early embryos could be linked to a membrane localization event. To explore whether a Xdsh membrane association event could take place during early *Xenopus* development, we tested several *Xenopus* Frizzleds for their ability to accumulate Xdsh at the membrane. Three recently isolated *Xenopus* homologs of the *frizzled* gene family (Xfz-3, Xfz-7 and Xfz-8) are expressed during early stages of *Xenopus* development (Deardorff *et al.*, 1998; Itoh *et al.*, 1998; Shi *et al.*, 1998). Overexpression of Xfz-8 in the ventral side of early cleavage embryos induces a secondary axis; in contrast, Xfz-3 and -7 fail to form an ectopic axis (Deardorff *et al.*, 1998). While Xdsh–green fluorescent protein (GFP) is evenly distributed in animal cap cells (Figure 2A), co-expression with rat Frizzled-1 but not rat Frizzled-2 accumulates Xdsh at the membrane
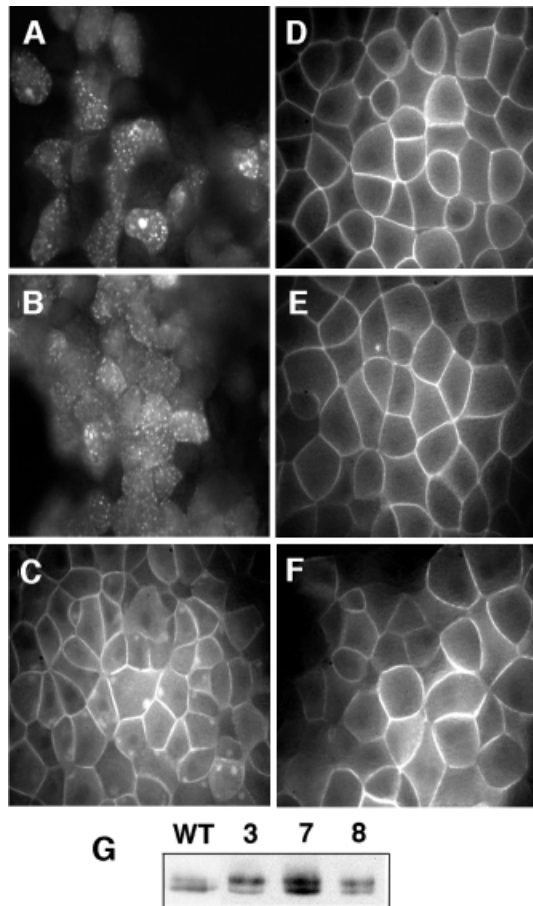
Fig. 2. *Xenopus* Frizzleds translocate and phosphorylate Xdsh independently of their axis-inducing abilities. *Xenopus* Frizzled-3, -7 and -8 can translocate Xdsh equally to the membrane; a comparison with rat Frizzled-1 and -2 is shown. (**A**) Ectopic Xdsh–GFP is distributed in a punctuate fashion in animal cap cells. (**B**) Co-expression of Xdsh–GFP with rat Frizzled-2 does not change its distribution. (**C**) Co-expression with rat Frizzled-1 leads to the accumulation of Xdsh–GFP near the cell membrane. Co-expression of (**D**) Xfz-3, (**E**) Xfz-7 and (**F**) Xfz-8 equally enriches Xdsh–GFP at the cell membrane. (**G**) Xfz-3, -7 and -8 can hyperphosphorylate Xdsh. Anti-myc staining of embryonic extracts is shown following injection of myc-Xdsh alone (WT) or after co-injection with Xfz-3 (3), Xfz-7 (7) or Xfz-8 (8).

(Yang-Snyder *et al*., 1996; and Figure 2B and C). In contrast, all three *Xenopus* Frizzleds tested accumulate Xdsh at the membrane (Figure 2D–F), irrespective of their ability to induce ectopic axes.

We further find that all three *Xenopus* Frizzleds cause Xdsh hyperphosphorylation (Figure 2G).

From these experiments, we conclude that the ability of Frizzled molecules to recruit Xdsh to the membrane and to cause its hyperphosphorylation is distinct from their axis-inducing ability, and that membrane association alone is not sufficient to activate the nuclear (β-catenin-mediated) signaling pathway. Because these Frizzleds are expressed early in development and can mediate Xdsh membrane accumulation, such an event may be important during early *Xenopus* development. The exact functional interplay between Frizzled-mediated membrane accumulation and phosphorylation of Xdsh during embryogenesis remains to be resolved.

The C-terminal region containing DEP is necessary and sufficient for Xdsh membrane accumulation

Various Xdsh deletion constructs were generated to examine the potential connections between Xdsh phosphorylation, Xdsh membrane association and axis formation, as well as to identify a role for each of the Xdsh domains (i.e. DIX, PDZ and DEP) in these events. Figure 3 summarizes the characterization of these deletion constructs.

First, the Xdsh deletion mutants were tested for their ability to accumulate at the membrane upon co-expression of rat *frizzled-1*. The various Xdsh mRNAs (40–400 pg) were injected in animal blastomeres of 2- or 4-cell stage embryos without (Figure 4A, C, E G, I and K) or with 1–2 ng of rat *frizzled* mRNA (Figure 4B, D, F, H, J and L). Animal caps were harvested from embryos grown to late blastula or early gastrula stage and then either mounted directly (for GFP-tagged constructs) or stained with anti-HA primary and fluorescent secondary antibodies and then mounted for fluorescence microscopy. Normally, Xdsh is distributed at various subcellular sites in the cells (Figure 4A). Co-expression with rat Frizzled-1 causes Xdsh membrane accumulation (Figure 4B). Deletions within DIX (D1) and a portion of PDZ (D4) strongly reduce the ability to translocate to the membrane but do not completely abolish it (Figure 4C and D, and G and H). Deletion of the C-terminal DEP-containing region of Xdsh (D5 and D6) completely abolishes membrane translocation (Figure 4I and J). In contrast, deletion of the entire PDZ domain (D2 and D3) does not significantly affect the membrane accumulation properties of Xdsh (Figure 4E and F). Because the above results suggest a requirement for the C-terminal region containing the DEP domain in Xdsh translocation to the membrane, we tested the sufficiency of this region of Xdsh to direct the membrane translocation. Injection of a minimal construct containing only the C-terminal region encompassing the DEP domain of Xdsh (D9) results in its moderate, but clear membrane accumulation (Figure 4K and L). Thus, the C-terminal region containing the DEP domain is both necessary and sufficient to mediate the membrane translocation of Xdsh and therefore contains the membrane anchor motif. However, since the DEP-directed membrane accumulation is not as efficient as that of wild-type Xdsh, other Xdsh regions are likely to contribute to the efficient translocation process.

Xdsh phosphorylation requires DEP-containing regions

Deletion mutants were analyzed on SDS–PAGE for their degree of phosphorylation. Embryos were injected with mRNAs (1–2 ng) at the 2- to 8-cell stages, grown to blastula or gastrula stages, and analyzed for the abundance of differentially migrating Xdsh protein forms. Mutations deleting the C-terminus of the DEP domain abolish the mobility shift (D5, not shown, and D6, Figure 5B), suggesting that this region is required for phosphorylation. In contrast, other deletions (D1 and D4, Figure 3) only reduce but do not eliminate Xdsh phosphorylation (Figure 5A). Deletion of the entire PDZ domain leaves Xdsh phosphorylation intact (D2, Figure 5A, and D3, not shown). Since D9 protein is neither recognized by anti-Dsh antibodies, nor stained well with anti-GFP antibodies,

Structure/Function Analysis of *Xenopus* Dishevelled
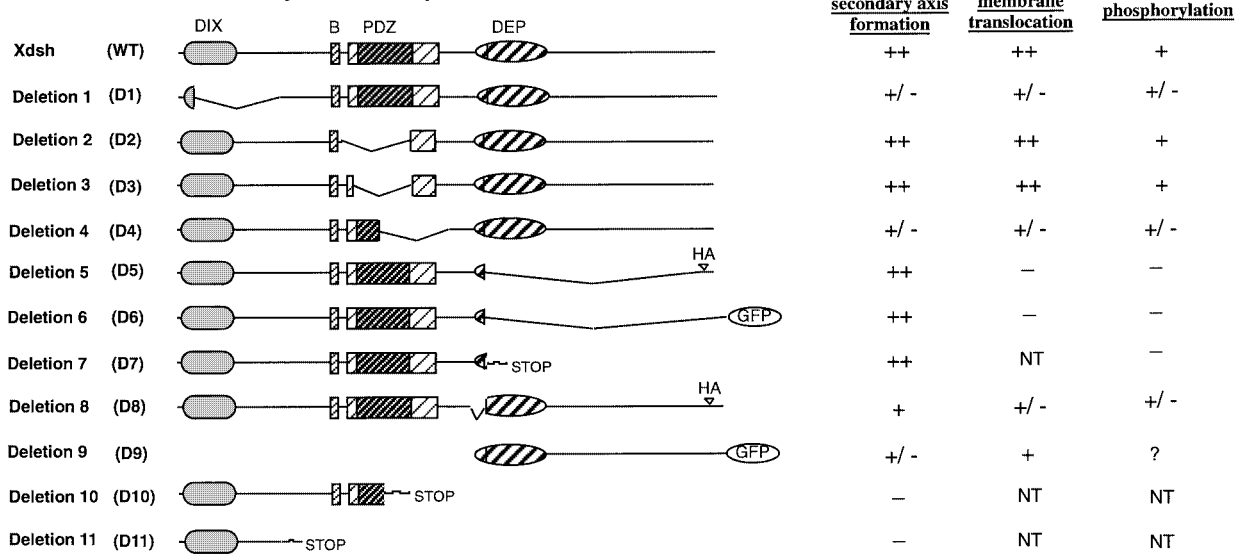
Fig. 3. Summary of the Xdsh structure–function analysis. Left panel: a schematic overview of the relative location of conserved domains in Xdsh (wild-type, WT) and those regions which are deleted in the individual mutant constructs (D1–D11). Regions conserved between *Drosophila* and vertebrates are shaded or stippled (DIX, B for basic region, PDZ and DEP; the globular core region of the PDZ domain is darkly shaded). All Xdsh constructs are epitope tagged near or at the C-terminus with HA or GFP tags, respectively, except those labeled with a STOP. HA or GFP labels are shown if only one tagged version was generated. WT, D1 and D4 were also generated as untagged constructs. Right panel: summary of the functions of Xdsh deletions assayed for membrane translocation, phosphorylation status or secondary axis formation, as shown in Figures 4–6. Semi-quantitative and qualitative differences are indicated as: –, no effect; +/–, weak effect or bent in secondary axis assay; +, clearly positive effect; ++, strong effect; ?, inconclusive; NT, not tested.

it is difficult to assess whether D9 is phosphorylated. Thus, we can only conclude that C-terminal regions encompassing the DEP domain contain either phosphorylation site(s) or a kinase-docking region. Both Xdsh membrane accumulation and phosphorylation depend on the presence of the DEP domain, raising the possibility that the two events are functionally connected.

Axis induction requires DIX and N-DEP regions

The functional significance of Xdsh membrane accumulation and phosphorylation in ectopic axis formation was examined by injection of Xdsh or mutant Xdsh mRNA (200 pg–2 ng) into one vegetal-ventral blastomere at the 8-cell stage. Embryos were grown to early neurula stage (stage 13) or tailbud stage (stage 42) and analyzed for secondary axis formation. Immunoblotting analysis of embryonic extracts isolated from each injected sample confirmed that nearly identical levels of proteins were expressed (data not shown). Figure 6H summarizes the ectopic axes generated after injection of the various Xdsh deletions used here. The most striking result is that DEP-deficient Xdsh deletions are able to induce complete secondary axes (including eyes and cement glands) similar to full-length Xdsh (Figure 6A and E). This is in dramatic contrast to the loss of membrane accumulation and phosphorylation by the same deletions. Other deletions eliminate (D10 and D11) or drastically reduce the extent of (D1, D4 and D8) secondary axis formation. For example, elimination of most of the DIX region (D1, Figure 6B) or elimination of half of the PDZ domain (D4, Figure 6D) significantly reduces axis formation, forming mostly single bent primary axes (presumably caused by fusion of a weak secondary axis together with a primary axis). Deletion of a short region in DEP (called N-DEP) allows the formation of incomplete secondary axes with prominent secondary neural tubes (Figure 6F). In contrast, deletion of the entire PDZ domain (D2 and D3, Figure 6C) retains the ability of Xdsh to induce complete secondary axes.

Taken together, these results suggest that PDZ and most of DEP are dispensable for secondary axis formation, while DIX is necessary. Additionally, regions in DIX, N-DEP and in PDZ may have a conformational significance since deletion within these domains causes defects in all three Dsh assays (axis formation, membrane accumulation and phosphorylation; see Figure 3 and Discussion).

Xdsh forms homomeric complexes in vivo

Previous studies demonstrated that Xdd1 (identical to D4 in our study) acts as a dominant-negative form to block ectopic Xdsh-induced axes. Inactivation by Xdd1/D4 may occur via homomeric interaction with full-length Xdsh or by titrating other proteins interacting with Xdsh. To analyze these possibilities, we examined homomeric interactions in co-translocation and co-precipitation assays *in vivo*.

First, we examined the ability of various Xdsh deletions that are defective in membrane accumulation to co-translocate to the membrane together with wild-type Xdsh. For this, we co-injected mRNA encoding full-length *Xdsh* and an *Xdsh* deletion, either with or without rat *frizzled-1*. Deletion mutants, unable or weakly able to associate with membranes when co-injected with rat *frizzled-1*, are now able to accumulate in membranes if co-expressed with wild-type Xdsh. As shown in Figure 7,

in the absence of *frizzled*, Xdsh-HA (Figure 7A) and D6–GFP (Figure 7B) are evenly distributed in the cells. Figure 7C shows an overlay of both signals (Xdsh-HA in the red and D6–GFP in the green channel). Following *frizzled* co-expression, both Xdsh-HA (Figure 7D) and D6–GFP (Figure 7E) become enriched at the membrane (Figure 7F shows an overlay, as above). Similarly, when D8-HA (Figure 7G) and Xdsh–GFP (Figure 7H) are co-injected together with *frizzled*, these proteins accumulated at the membrane (Figure 7G–L). D1, D4 and D5 also behaved in a similar manner (not shown). These data indicate that mutant and wild-type Dsh can interact (directly or indirectly) and form a stable complex that co-translocates to the membrane. Because the DEP-deficient Dsh alone (D6) completely fails to associate with the

membrane (Figure 4I and J) but co-translocates with full-length Xdsh (Figure 7A–F), we conclude that Xdsh membrane accumulation does not depend on the pairing of DEP domains. Taken together, these findings strongly suggest that Xdsh can form homomeric complexes *in vivo* via N-terminal regions.

To determine directly whether Xdsh can form homomeric interactions, co-immunoprecipitation assays were performed using differently epitope-tagged Xdsh. Xdsh-HA and myc-Xdsh were expressed alone or co-expressed together in embryos and subjected to immunoprecipitation analysis with anti-myc antibody. Western blots were first stained with anti-HA monoclonal antibody and subsequently with anti-myc antibody to detect the presence of both Xdsh-HA and myc-Xdsh in individual samples. Figure 8 shows that in co-injected embryos, immuno-precipiation of myc-Xdsh (100 kDa, lane 6) results in co-immunoprecipitation of Xdsh-HA (85 kDa, lane 3). Longer
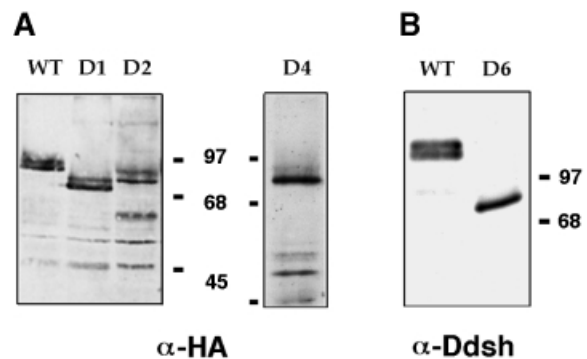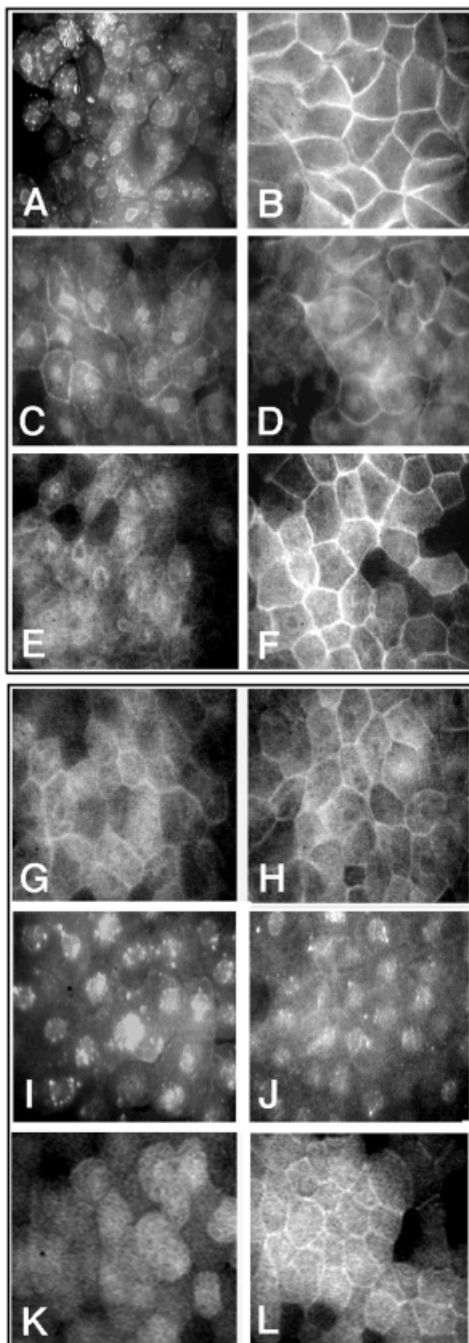
Fig. 5. Phosphorylation status of Xdsh deletions. (**A**) mRNA for HA-tagged Xdsh or deletions was injected in one animal blastomere at the 8-cell stage. An anti-HA stain of an equivalent of two blastula or early gastrula extracts per lane shows that all deletions show at least two bands, where the more slowly migrating (upper) band constitutes the phosphorylated form (deletions indicated at the top of each lane, WT, D1–D2; D4 is from a separate gel. (**B**) Blot of Xdsh–GFP and C-terminal truncation deletion D6–GFP stained with anti-Ddsh antiserum. Note that D6, which was shown to induce secondary axes (Figure 6E), is poorly or not phosphorylated.

Fig. 4. Translocation abilities of Xdsh–GFP deletions upon rat *frizzled-1* co-expression: the C-terminal DEP domain-containing region is necessary and sufficient for Xdsh membrane translocation. (**A**) Xdsh localizes in various subcellular regions of animal cap cells in punctuate appearance resembling vesicular structures. These are distributed in the cytoplasm, at the membrane and around the nucleus. (**B**) Upon *frizzled* co-expression, Xdsh is localized prominently at the membrane. Almost no Xdsh is seen in cytosolic locations. (**C**) D1, which lacks much of the DIX domain and flanking regions, is distributed similarly within the cell and shows less obvious accumulation than Xdsh in vesicles. (**D**) D1 translocates poorly to the membrane upon *frizzled* co-injection. (**E**) D2, which lacks the entire PDZ domain, is distributed in the entire cell, and (**F**) upon *frizzled* co-injection is localized prominently to the membrane. (**G**) D4, which lacks half of the PDZ domain, is distributed evenly in cells; (**H**) *frizzled* co-expression can mediate its membrane localization only to a very small extent. (**I**) D6 lacks the C-terminal region containing most of the DEP domain and localizes prominently to punctuate accumulations within the cells. (**J**) This cellular distribution of D6 does not change upon *frizzled* injection, and no membrane localization is observed. (**K**) D9, containing only the C-terminal region of Xdsh encompassing the DEP domain, shows mainly a cytoplasmic distribution. (**L**) *frizzled* co-expression clearly can promote D9 accumulation at the membrane.
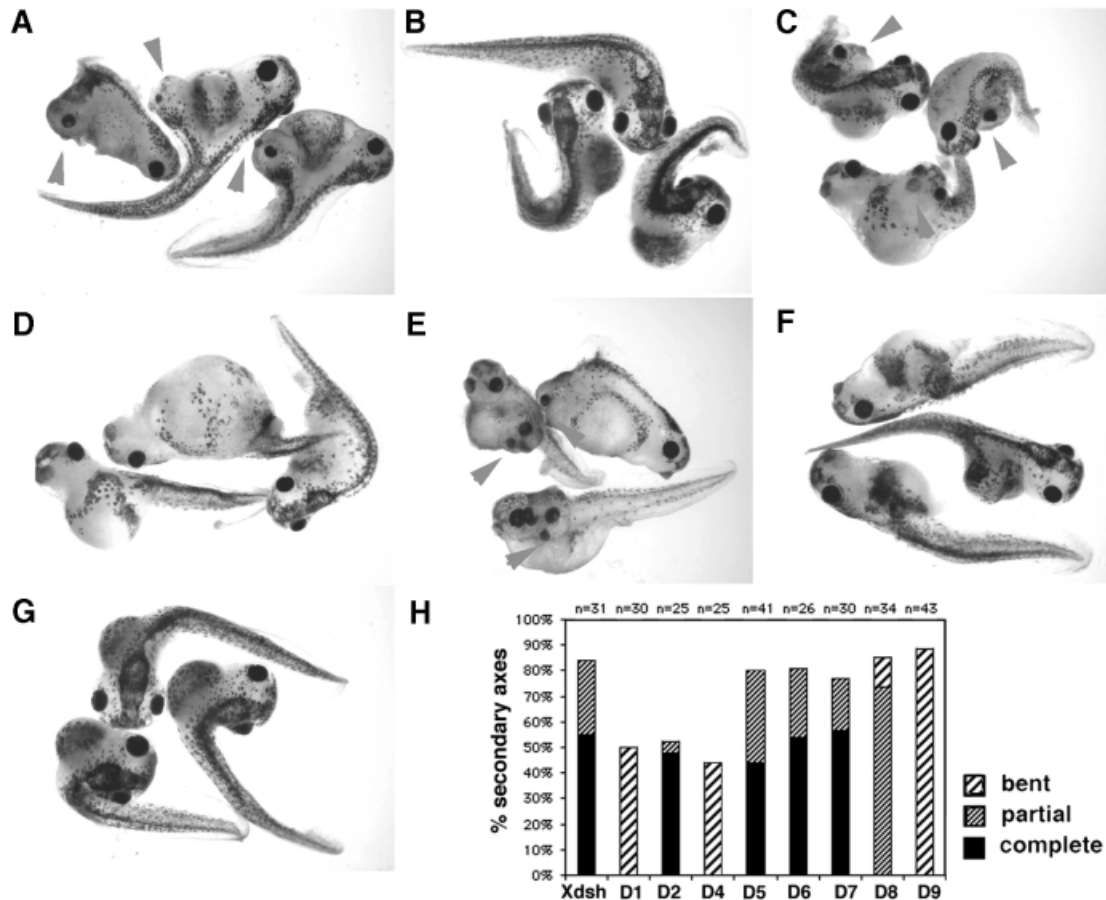
Fig. 6. Axis induction abilities of Xdsh deletions: the PDZ domain and most of the DEP domain are dispensable, the DIX region and N-DEP are essential. At the 8-cell stage, one ventral-vegetal blastomere was injected with between 200 pg and 2 ng of mRNA and scored between stages 13 and 42 for secondary neural tubes and secondary heads, eyes and cement glands. Representative embryos that were injected with 1 ng of mRNA are shown: (**A**) Xdsh-WT; (**B**) D1, deletion in the DIX domain; (**C**) D2, deletion of the entire PDZ domain; (**D**) D4, partial deletion of the PDZ domain; (**E**) D6, C-terminal deletion lacking most of DEP; (**F**) D8, selective deletion of N-DEP; and (**G**) D9, C-terminal region only, containing DEP. (**H**) The relative degree of secondary axes induced by various deletion versions of Xdsh is shown: in black is the percentage of complete secondary axes, dense hatching represents the percentage of incomplete or partial secondary axes, wide-spaced hatching represents the percentage of embryos with bent axes or very weak secondary axes, and unlabeled is the amount of other phenotypes, including normal or developmentally defective embryos. Numbers D1–D9 are from a single representative experiment, Xdsh is a compilation of three different injections.

electrophoresis runs (see anti-Ddsh stain, Figure 8) confirmed the presence of two migrating forms (phosphorylated and unphosphorylated) of both HA- and myc-Xdsh.

Thus, the biological and biochemical data presented here support the hypothesis that Xdsh forms stable homomeric complexes, in both the presence and absence of Frizzleds. A recent study by Kishida *et al.* (1999), on mouse Dishevelled, independently confirms our results.

Discussion

Dishevelled protein in the embryo

We find that *Xenopus* Dsh protein is phosphorylated differentially during early development. More importantly, the Xdsh phosphorylation is significantly higher in the dorsal half of early cleavage stages and correlates in time and place with the onset of dorsalizing events in the embryo. Differential Xdsh phosphorylation, together with the dorsal β-catenin accumulation, is the earliest molecular manifestation of events that break the radial symmetry in the embryo. This result suggests that current models of dorso-ventral patterning may require modifications (for a review see Miller and Moon, 1996). The first signs of

cytoplasmic β-catenin accumulation are detected in 2-cell stage embryos, while nuclear accumulation of the protein is seen only after several rounds of cleavages (Schneider *et al.*, 1996; Larabell *et al.*, 1997). We detect Xdsh phosphorylation in Western blots by the 16-cell stage, presumably after onset of β-catenin accumulation but possibly before or at the time of its nuclear accumulation (the 16- to 32-cell stage). Due to insufficient sensitivity of our detection method, Xdsh phosphorylation onset may occur earlier. Three possible scenarios can therefore interpret our Xdsh localization and phosphorylation result. First, phosphorylation of Xdsh leads to the activation of the downstream Wnt signaling pathway and dorsal (nuclear) β-catenin accumulation. Secondly, Xdsh phosphorylation is a result of β-catenin accumulation. Finally, the phosphorylation of Xdsh and nuclear β-catenin accumulation are unlinked. A very recent study demonstrates accumulation of Xdsh protein itself in dorsal regions, caused by cytoskeletal transport following cortical rotation (Miller *et al.*, 1999). It is important to note that we further detect significantly more phosphorylated than unphosphorylated Xdsh protein in the dorsal side even after considering the enrichment of Xdsh protein in the dorsal region, indicating
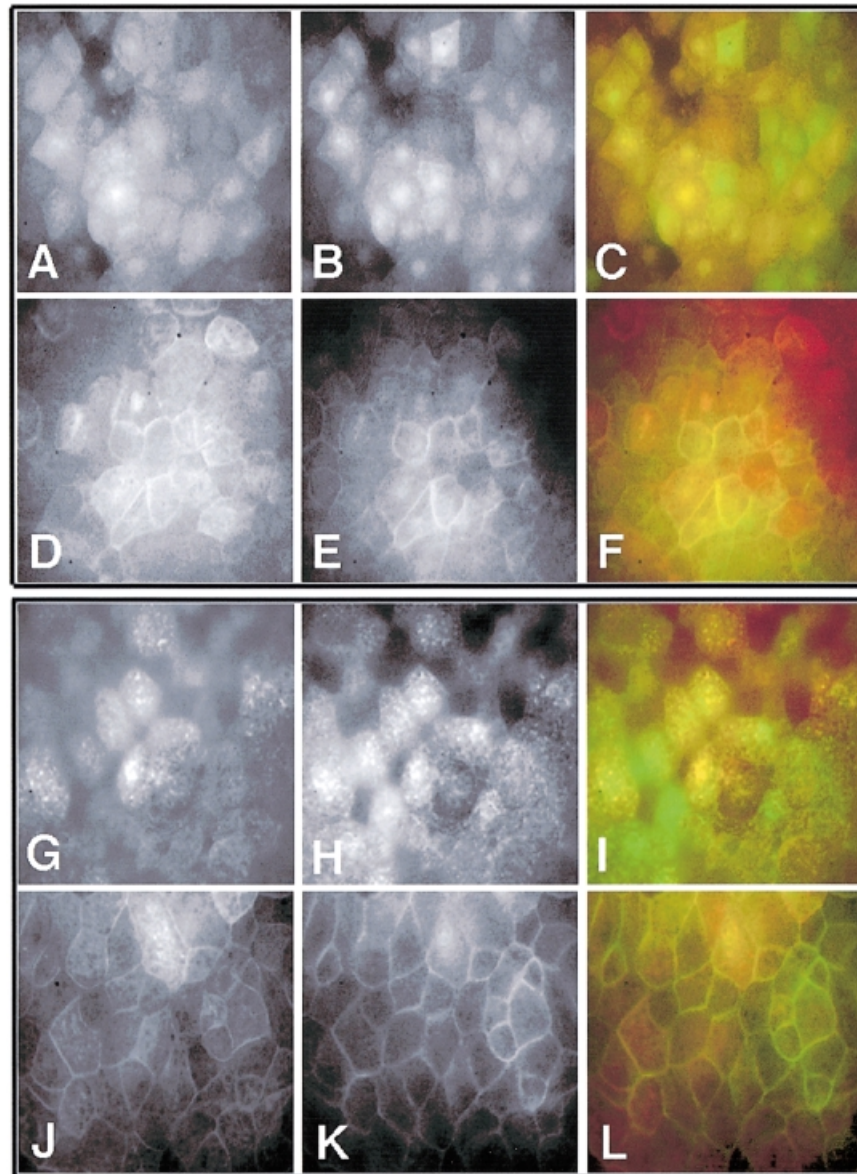
Fig. 7. Homomeric complex formation of Xdsh: membrane co-translocation of translocation-defective deletions with wild-type Xdsh. mRNAs for Xdsh-HA (A and D) and D6–GFP (B and E) were co-injected in early stage embryos without (A–C) or with rat *frizzled-1* mRNA (D–F). The subcellular location of mutant and wild-type Xdsh in gastrula animal caps is shown. Images on the left (**A** and **D**) show the fluorescence of rhodamine-labeled Xdsh-HA (red channel), middle images (**B** and **E**) show the GFP fluorescence of D6–GFP (green channel) in the same animal cap tissue; and images on the right (**C** and **F**) are overlays of both signals. Note that D6–GFP (E) is found associated with the membrane when it is co-injected with Xdsh-HA and *frizzled*, while it remains cytoplasmic/vesicular when co-injected with *frizzled* alone (compare Figure 4J). D8-HA (G and J) co-injection with Xdsh–GFP (H and K) results in D8-HA accumulation at the membrane, when co-injected with *frizzled* (J–L). D8 on its own with *frizzled* does not localize well to the membrane (data not shown). Left panels (red channel) are Texas red signals of D8-HA (**G** and **J**); middle panels (green channel) are GFP signals (**H** and **K**) and right panels are overlays of both signals (**I** and **L**).

that phosphorylation *per se* is important, in addition to or independently of Xdsh accumulation.

Several lines of evidence indicate that phosphorylation of Dsh may be a result of Frizzled activation. Frizzled molecules are putative Wnt receptors (Bhanot *et al.*, 1996) and are required in the Wnt signaling pathway (Bhat, 1998; Kennerdell and Carthew, 1998; Müller *et al.*, 1999). When overexpressed, Frizzleds are able to both enhance Dsh phosphorylation and promote the membrane accumulation of Dsh (Yanagawa *et al.*, 1995; Semenov and Snyder, 1997; our results). As Wnt factors themselves can also induce phosphorylation of

Drosophila Dsh or mouse Dvl (Yanagawa *et al.*, 1995; Willert *et al.*, 1997; Lee *et al.*, 1999), Dsh phosphorylation appears to be linked to the activation of the Wnt pathway and is therefore expected to be higher at the site of Wnt pathway activation in the embryo. Two recent studies describe a role for CKIε in Wnt signaling, while CKIε associates and phosphorylates Xdsh (Peters *et al.*, 1999; Sakanaka *et al.*, 1999). Less clear, however, is the downstream consequence of Xdsh phosphorylation, whether it is required for Wnt pathway activation, or whether it has other consequences. Our deletion analysis aims to answer some of these questions.
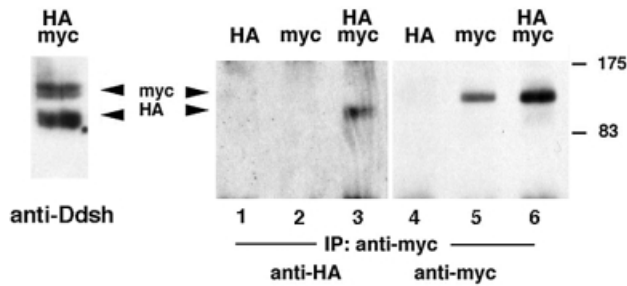
Fig. 8. Biochemical detection of Xdsh homomeric complexes: co-immunoprecipitation of Xdsh-HA and myc-Xdsh. Embryos were injected with either Xdsh-HA (lanes 1 and 4), myc-Xdsh (lanes 2 and 5) or both (lanes 3 and 6) and precipitated with anti-myc antibody, then Western blotted. The blot was first stained with anti-HA antibody (left panel, lanes 1–3), followed by peroxidase inactivation, and restained with anti-myc antibody (right panel, lanes 4–6). Anti-myc antibody precipitates myc-Xdsh of 100 kDa from myc-Xdsh-injected and from co-injected embryos (arrowhead labeled myc in lanes 5 and 6) but not from Xdsh-HA-injected embryos (lanes 1 and 4). Xdsh-HA of 85 kDa (arrowhead labeled HA, lane 3), however, is co-precipitated with anti-myc antibody from embryos co-injected with myc- and HA-tagged Xdsh. The left panel shows an anti-Ddsh stain of longer run myc co-precipitates revealing that both HA and myc-Xdsh contain multiple (phosphorylated) forms. The top of the Figure indicates the mRNA injected: HA is Xdsh-HA, myc is myc-Xdsh, HA/myc is co-injection of Xdsh-HA and myc-Xdsh; the bottom of the Figure shows that anti-myc antibody was used for immunoprecipitation (IP), and staining performed with anti-HA (lanes 1–3) and anti-myc (lanes 4–6) or anti-*Drosophila* Dsh antibodies (anti-Ddsh, left panel). Standard molecular weights are indicated on the right.

Uncoupling of Xdsh characteristics by deletion analysis

Our deletion analysis using overexpression assays suggests that the Xdsh phosphorylation and membrane accumulation can be functionally uncoupled from Dsh-mediated axis formation. We propose a model (Figure 9) where Xdsh mediates its functions by interacting with different sets of molecules via different domains. DEP domain regions mediate the Xdsh membrane association and are linked to phosphorylation of Xdsh, suggesting a functional interdependency of the two events. The DIX domain, together with a short stretch at the N-terminus of the DEP, is important for secondary axis formation but can also influence membrane accumulation and phosphorylation of Xdsh. The PDZ domain, in contrast to what was believed previously, is not required for either ectopic axis formation or membrane association. However, the results suggest that the PDZ domain may play an important role in the tertiary structure of Xdsh, possibly by linking the DIX and N-DEP regions together to form a functional unit (discussed further below). Finally, our deletion analysis uncovered that Xdsh can form a multimeric complex, raising the possibility that complex formation is necessary for proper Xdsh functions. Thus, when using ectopic Xdsh assays, we need to keep in mind that ectopic Xdsh may influence axis formation by interacting with and modifying endogenous Xdsh.

Dishevelled membrane association and phosphorylation require the DEP domain. We show that DEP domain-containing regions are necessary and sufficient for the Frizzled-mediated membrane association of Xdsh. Thus, Xdsh behaves similarly to *Drosophila* Dsh assayed in *Xenopus* (Axelrod *et al.*, 1998). However, we also show
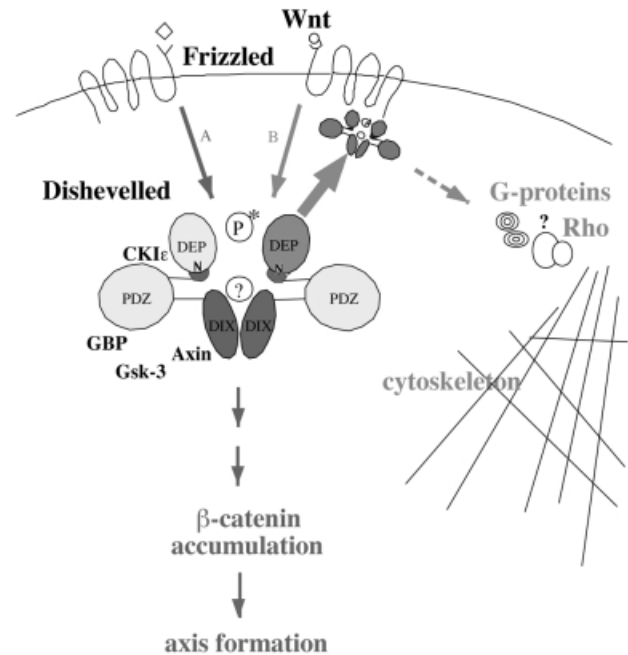
Fig. 9. Model of Xdsh domains mediating Wnt signaling and its role at the membrane. Wnt signaling components and the putative transducing domains in Xdsh are indicated in dark gray; the membrane translocation domain of Xdsh, the incoming putative tissue polarity signal as well as possible effects are depicted in light gray. Specific Wnt molecules bind and trigger the Frizzled receptors to transmit their respective intracellular signals (A or B, or both). Xdsh integrates different signals from Frizzled receptors and mediates a β-catenin-dependent pathway (**A**, dark gray) and a tissue polarity-like pathway (**B**, light gray), or both. Xdsh is modified via a kinase (P*). The DEP domain regions mediate the Xdsh accumulation at the membrane, which may lead to the regulation of G-protein signaling and Rho-mediated cytoskeletal rearrangements. The DIX region and the small N-DEP stretch of Xdsh may be brought into proximity by the PDZ domain and act in concert to transduce the Wnt signaling cascade that leads to β-catenin accumulation and nuclear signaling necessary for axis formation. Newly discovered Xdsh-interacting molecules (CKIε, axin, GBP and, indirectly, GSK-3) are indicated near the interacting Xdsh region.

that membrane association of Xdsh is not sufficient for secondary axis formation to occur: various *Xenopus* Frizzleds with differential abilities to induce a secondary axis can all accumulate Xdsh at the membrane. Interestingly, DEP regions are also required for Xdsh phosphorylation, suggesting a functional link to membrane association. Xdsh phosphorylation, like membrane accumulation, may not directly induce the activation of the β-catenin-mediated Wnt pathway (axis formation), since they are both dispensable for axis induction in overexpression experiments. It is possible, however, that phosphorylation of Xdsh at the membrane causes important activity changes of endogenous Xdsh. In *Drosophila*, Dfz-2-mediated Dsh phosphorylation via casein kinase II (CKII) is similarly insufficient to induce accumulation of Armadillo, a *Drosophila* homolog of β-catenin (Willert *et al.*, 1997). In contrast, CKIε overexpression in *Xenopus* leads to both Dsh phosphorylation and downstream pathway activation (Peters *et al.*, 1999; Sakanaka *et al.*, 1999), suggesting that CKIε might be important for the nuclear Wnt signaling activation. It remains to be determined whether CKIε is the kinase which causes the dorsally enriched Xdsh phosphorylation and whether DEP regions

are involved. Interestingly, the DEP domain of Egl-10 in *C.elegans* is sufficient to target the molecule to membranous subcellular compartments (Koelle and Horvitz, 1996). It needs to be determined whether vesicle-mediated transport of Xdsh to the dorsal side following cortical rotation (Miller *et al.*, 1999) is also DEP and/or phosphorylation dependent.

Accumulating evidence suggests that Dsh-mediated Wnt signaling not only affects nuclear signaling mediated via β-catenin and Lef/Tcf, but is also involved in providing cell polarity, possibly by regulating G-protein functions. The role of Frizzled or Dsh in G-protein signaling has been suggested in *Drosophila* (Adler *et al.*, 1997; Strutt *et al.*, 1997; Axelrod *et al.*, 1998; Boutros *et al.*, 1998, Gho and Schweisguth, 1998) and zebrafish (Slusarski *et al.*, 1997), raising the possibility that Dsh in *Xenopus* may play some similar role during embryogenesis, perhaps by influencing the formation of cytoskeletal structures in their establishment of dorsal–ventral differences in early amphibian embryos. Recent studies in *Drosophila* further demonstrate how small Frizzled and Dsh signaling differences can generate binary cell fate decisions in the eye (Cooper and Bray, 1999; Fanto and Mlodzik, 1999).

The roles of DIX and PDZ regions. The PDZ domain and most of the DEP domain (mediating membrane translocation) are dispensable for axis formation, while the DIX domain-containing region, possibly in conjunction with the short N-DEP stretch, may play a more direct role in axis induction. A recent study on mouse Dvl-1 (Moriguchi *et al.*, 1999) reaches similar conclusions concerning the involvement of the DIX domain in axis formation. Interestingly, DIX regions in Dsh recently have been implicated in axin binding (Fagotto *et al.*, 1999; Kishida *et al.*, 1999; Smalley *et al.*, 1999), supporting the idea that ectopic Dsh may activate downstream Wnt signaling by influencing the balance of an axin-containing complex which normally inhibits Wnt signaling. This could explain how deletion mutants deficient in membrane localization or phosphorylation (lacking DEP but containing DIX) maintain axis-forming abilities by interacting with axin.

In contrast, the PDZ domain, which previously was proposed to be required for Wnt signaling (Yanagawa *et al.*, 1995; Sokol, 1996), is dispensable for axis induction in our study. This may be explained when considering the putative structural role of the PDZ domain which separates the DIX domain from the N-DEP stretch within Dsh. Crystal structural analysis of PDZ domains reveals a strong tertiary structure, where the N- and C-terminal ends of this domain are in close proximity, forming a globular unit (Cabral *et al.*, 1996; Doyle *et al.*, 1996). Thus, the tertiary conformation of the PDZ domain would be expected to bring together the N-DEP and the DIX domains, perhaps to form a functional unit. In such a case, any partial deletion of the PDZ domain is likely to disrupt this structural integrity, thereby weakening their ability to mediate Wnt signaling. In contrast, complete deletion of the PDZ domain may recreate a fully active Dsh molecule (as shown in the present work) by bringing together DIX and N-DEP domains. Interestingly, in *C.elegans* Cdvl-1, the conserved, Dsh-specific N-DEP stretch (PD/ES/TGLEV/IR/K) is fused to the DIX domain

(see sequence alignment in Semenov and Snyder, 1997), supporting the hypothesis that the conjunction of the DIX domain and the N-DEP domain might be necessary for a functional signaling unit. As a result, previous investigations of Dsh may have concluded incorrectly on a critical role for the PDZ itself in mediating the β-catenin pathway as well as in the action of dominant-negative Dsh Xdd1/D4 (Yanagawa *et al.*, 1995; Sokol, 1996). Besides its conformational importance, the PDZ domain may play other more direct roles. Recently, CKIε binding was proposed to occur via regions missing in Xdd1 (Peters *et al.*, 1999). As half the PDZ domain and flanking regions are missing in Xdd1, it is possible that CKIε is the endogenous Xdsh kinase that binds via the PDZ and/or flanking regions and causes Xdsh phosphorylation *in vivo*. Additionally, GBP/Frat1, identified due to its GSK-3 binding, was shown recently to bind the Xdsh PDZ domain (Li *et al.*, 1999b). Understanding of the intricate multiprotein interactions of Dsh, axin, GBP, GSK-3 and CKIε in regulating Xdsh functions and downstream Wnt signaling requires further characterization.

Multimer formation of Dishevelled and its implications. Both co-expression and co-translocation assays indicate that Xdsh forms homomeric complexes *in vivo*. Our data do not exclude the possibility that this interaction is indirect and that other molecules participate in the formation of multimeric Dsh complexes. The formation of Xdsh multimeric protein complexes is significant for the interpretation of results where ectopic Xdsh is likely to interact with endogenous Xdsh pools. Previous studies have demonstrated that a partial deletion of the PDZ domain results in the generation of a dominant-negative Xdsh protein (equal to D4 in our study) that inhibits ectopic axis formation of overexpressed Xdsh but fails to inhibit normal body axis formation (Sokol *et al.*, 1995). This result led to the idea that Xdsh is not involved in primary axis formation, i.e. the stabilization of β-catenin immediately after fertilization. However, based on our finding that Dsh can form homomeric complexes and that the majority of this PDZ-defective Xdsh fails to translocate to the membrane, we suggest that it may interfere mainly with the function of cytoplasmic Xdsh. Membrane-associated pools of Xdsh already pre-engaged in stable complexes may not be dissociated readily by ectopic dominant-negative Xdsh, reminiscent of the reported failure of dominant-negative activin to block endogenous dimeric activin (Wittbrodt and Rosa, 1994).

The role of Xdsh during endogenous axis formation

Only one Dsh molecule has been found so far in *Xenopus* (our unpublished observation; for details, see Materials and methods), and Xdsh may represent the obligatory component through which Frizzled molecules mediate their function(s) in *Xenopus*. During embryogenesis, distinct Frizzled molecules may instruct Xdsh to activate either a β-catenin-dependent or -independent pathway, or both (Bhat, 1998; Deardorff *et al.*, 1998; Itoh *et al.*, 1998; Kennerdell and Carthew, 1998; Müller *et al.*, 1999; Shi *et al.*, 1998). So far, three maternally expressed *Xenopus* Frizzled proteins (Xfz-3, -7 and -8) have been identified in *Xenopus*. We show that they all can translocate Xdsh

to the membrane; in contrast, only Xfz-8 can induce a secondary axis (Deardorff *et al.*, 1998). Xfz-7 is expressed most abundantly in early cleavage stages (M.A.Deardoff and P.S.Klein, unpublished) and thus may function as a primary anchor to recruit endogenous Xdsh to the membrane. Initial phosphorylation of Xdsh soon after fertilization may reflect such membrane association events. At present, it is unclear how differential Xdsh phosphorylation is achieved in the embryo One possibility is that as yet unidentified Wnt-like growth factors activate the Frizzled receptor system. A recent study in zebrafish supports this hypothesis, since a dominant-negative Fz blocks endogenous D/V signaling (Nasevicius *et al.*, 1998). Alternatively, Xdsh in early embryos might be activated *de novo* by a dorsally activated kinase in a Frizzled-independent manner. While our deletion analysis shows that different domains are involved in phosphorylation and membrane association versus axis formation, the exact mechanisms by which the activity of Xdsh is regulated in the embryo remain to be determined. In particular, the way in which phosphorylation may influence axis formation or other early events, including polarity of cells in the developing embryo, is still unclear. Two independent pieces of evidence clearly support our idea that endogenous Xdsh and possibly its phosphorylation are actually important in dorso-ventral patterning. First, CKIε causes Xdsh phosphorylation while being involved in Wnt signaling and is thus a good candidate for the endogenous Xdsh phosphorylation (Peters *et al.*, 1999; Sakanaka *et al.*, 1999). Interactions of Dsh and CKIε with axin and the GBP–GSK-3 complex suggest that the regulation of Dsh via phosphorylation or segregation to the membrane may be important factors in the activation of axis formation. Thus, while membrane association and phosphorylation normally may be required to regulate endogenous Dsh activities, in overexpression, a membrane association-and phosphorylation-deficient Dsh may cause axis formation by influencing the balance of this multiprotein complex. Secondly, the demonstration of active transport of Xdsh to the dorsal side (Miller *et al.*, 1999) additionally supports our hypothesis that Xdsh is involved in dorsal–ventral patterning.

For Dsh to be clearly implicated in activating the downstream Wnt signaling pathway in the embryo, it has to meet several criteria: Dsh protein should be present and active at the correct time and place in the embryo. In addition, activation of Dsh function should induce secondary axes, while blocking its activity should block primary axis formation. Here we present new evidence that maternal Dsh RNA is translated into a protein product, which is present throughout early cleavage stage embryos. Furthermore, Dsh protein becomes phosphorylated in a dorsal location at the appropriate time and place, correlating well with the initiation of dorso-ventral axis specification and the translocation of β-catenin to nuclei. Such activation of members of the Wnt signaling pathway was shown to lead to axis formation, and ectopic expression of Dsh itself induces secondary axis formation. Our results suggest that endogenous Xdsh is present in multimeric complexes. Because such pre-arranged multimers may not be destabilized and inactivated by dominant-negative forms, the evidence previously offered for lack of need for Xdsh is inconclusive. The evidence presented here

therefore revives the possibility that Xdsh is indeed involved in endogenous axial patterning.

Materials and methods

Xdsh expression constructs

Cloning of Xdsh was performed using primers annealing to regions conserved between *Drosophila* and mouse *Dsh* (encoding amino acids PCFNGR and AKCWDP, primers were: 5′TGCCGTGCTTTAATGG/ACCG3′ and 5′GGTCCCAGCATTTGGCCAC3′). A 800 bp PCR fragment obtained by RT–PCR from *Xenopus* gastrula stage RNA was used for screening *Xenopus* oocyte, egg, gastrula and head phage cDNA libraries. The *Xdsh* cDNA sequence obtained is largely identical to the subsequently published *Xdsh* sequence, DDBJ/EMBL/GenBank accession No. U31552, and differs in 13 positions, therefore probably reflecting either sequencing errors or tetraploidity variations of *Xdsh*. For expression in *Xenopus* embryos, a blunted 2190 bp *Xdsh Bfa*I fragment (encoding all except eight amino acids at the C-terminus of Xdsh) was cloned into the blunted *Bal*I–*Bst*EII sites of the Sp64T/Xβm vector (obtained by *Bal*I–*Bsp*EII excision of noggin-coding regions from the Xβnog vector obtained from R.Harland), called Xdsh-Xβm. An HA tag was introduced into an *Nco*I site close to the C-terminus. GFP tagging was performed using a modified pCS2-GFP vector (D.Turned, R.Rupp and H.Weintraub, Fred Hutchinson Cancer Research Center, Seattle, WA) encoding an enhanced version of GFP (obtained from C.LaBonne) and blunt cloning of a *Hin*dIII–blunt *Xho*I fragment and an *Xho*I–*Stu*I-cut PCR fragment into the blunted *Eco*RI site in-frame with the GFP-coding sequence, thus giving rise to full-length Xdsh with GFP fused to its C-terminal end. The *Bsp*EI–*Stu*I-cut PCR fragment was generated using the primers 5′GGAGGCCTCATGACATCCACAAAGAAC3′ and 5′GGGCGGCC-GTTCTCAAAATTAATGTC3′. Xdsh and deletion constructs (below) were sequenced to confirm correct cloning sites and sequences within PCR fragments. The following deletion constructs were generated: D1 (missing DIX and flanking regions) was generated by excision of an *Ssp*I–*Fsp*I fragment (bp 124–442 deleted), fusing amino acids ASHAK to (C)RDRVR. D2 (missing the PDZ domain) was generated by cloning a *Hin*dIII–*Apa*I-cut PCR fragment in *Hin*dIII–*Apa*I-cut Xdsh-HA vector using primer 5′ATGGGCCCCGTCC GTTCCAGGCGC3′ (bp 707–990 deleted), thus fusing amino acids RLERT to GPIVL. D3 (missing most of the PDZ domain) was generated by cloning a *Hin*dIII–*Apa*I-cut PCR fragment in *Hin*dIII–*Apa*I-cut Xdsh-HA vector using primer 5′ATGGCCCCACGATGGAGATG3′ (bp 806–990 deleted), fusing amino acids GISIV to GPIVL. D4 (missing half the PDZ domain) was generated by excision of a *Sma*I fragment (bp 894–1134 deleted), fusing amino acids GRIEP to GSASM. D5 (missing most DEP and C-terminal regions, HA tagged) was generated by excision of an *Xho*I–*Nco*I fragment (bp 1287–2164 deleted); the five most C-terminal amino acids of N-DEP are PESGL(D) followed by the HA tag and amino acids MGNP, vector sequences provide the STOP codon. D6 (missing most DEP and C-terminal regions, GFP tagged) was generated by *Apa*I–*Eco*RI digestion of a PCR fragment generated with primers SP6 and 5′GGGAATTCTCT-CGGACCTCGAGGC3′ ligated in *Apa*I–*Eco*RI sites of Xdsh–GFP (bp 1287–2202 deleted, bp 1–1286 maintained); the C-terminal Xdsh-coding amino acids are LEVRD, followed by GFP-coding sequences. D7 (missing most DEP and C-terminal regions, out-of-frame), is an out-of-frame construct which maintains bp 1–1286 of Xdsh (the C-terminal coding amino acids are PESGL) with a STOP codon further downstream, and contains 16 additional amino acids (DRSSGSGWGRLEVGIW) generated by frameshift. D8 (missing the N-terminal region within the DEP domain) was generated by *Apa*I–*Xho*I digestion of a PCR fragment generated by primers SP6 and 5′ACCTCGAGAGCCATGACCTT-CACAAC3′ and cloning into *Apa*I–*Xho*I-cut Xdsh-HA vector, resulting in a five amino acid deletion (amino acids SPESG, bp 1271–1286). D9 (missing all Xdsh regions upstream of the DEP domain, therefore missing DIX and PDZ but maintaining DEP) was generated by *Cla*I–*Bsp*EI digestion of a PCR fragment generated with primers 5′GGATCGAT-CCATGGCTTCTGTTGTGAAGG3′ and 5′GGGAATTCTCTCGG-ACCTCGAGGC3′ and cloning into *Cla*I–*Bsp*EI-cut Xdsh–GFP vector. Therefore, the most N-terminal coding amino acids are (M)ASVVK. D10 (truncation missing half of PDZ and all C-terminal regions, also DEP) is an out-of-frame construct, which maintains bp 1–893 of Xdsh; the most C-terminal coding amino acids are GRIEP followed by antisense sequences. D11 (truncation missing all middle and C-terminal regions, DIX maintained) is an out-of-frame construct which maintains bp 1–450 of Xdsh; the most C-terminal coding amino acids are SMRRD followed by out-of-frame amino acids.

Microinjection of synthetic RNA into fertilized eggs

Synthetic RNA was transcribed using the SP6 mMessage Machine Kit (Ambion) according to the manufacturer's recommendations. Injections and handling of embryos were as described previously (Blitz and Cho, 1995). For the secondary axis assay, 1 ng of Xdsh or mutant Xdsh mRNA was injected in one vegetal-ventral blastomere at the 8-cell stage and scored for phenotypes after stage 15. The induced phenotypes were scored by the presence of secondary neural tubes, heads and cement, and termed weakly dorsalized/bent when embryos were bent and sometimes had short secondary neural tubes (+/– in Figures 3 and 6B, D and G), partial secondary axis when a secondary neural tube but no eyes or cement gland were visible (+ in Figures 3 and 6F), complete secondary axis when a secondary neural tube and head including eyes and cement gland were present (+ + in Figures 3 and 6A, C and E) or hyperdorsalized when supernumerary eyes and cement glands were visible. For immuno-precipitations and immunoblotting, 1–2 ng of mRNA was injected per embryo. Phosphatase treatment was performed (Yanagawa *et al.*, 1995) using potato acid phosphatase (PAP) from Sigma. Full color documentation of embryos was performed using a Zeiss Axiophot dissecting microscope equipped with a Leica camera or a ProgRes 3012 digital color camera and ImageManager software (Roche Image Analysis Systems).

Immunoblotting and antibodies

Ten *Xenopus* embryos were homogenized in 200 µl of RIPA buffer (150 mM NaCl, 50 mM Tris pH 8, 1% NP-40, 0.5% sodium deoxycholate, 0.1% SDS) or NP-40 buffer (150 mM NaCl, 50 mM Tris pH 8, 1% NP-40). Cell debris was removed by centrifugation at 15 000 *g* for 10 min. Immunoprecipitations were performed using protein A–Sepharose beads or GammaBind G–Sepharose (Pharmacia) as described previously (Hawley *et al.*, 1995) using anti-HA antibody (12CA5, Berkeley Antibody Company) or anti-myc antibody (Oncogene Science). Alternatively, a crush method was used to detect both endogenous and overexpressed Xdsh from embryonic extracts (Watabe *et al.*, 1995). Briefly, 3–20 embryos in 25 µl of 0.1× MMR between stages 0 and 11 were centrifuged for 3 min at 15 000 *g* to remove yolk platelets. Yolk platelets and Xdsh protein migrate at a similar molecular weight in SDS–PAGE. Comparable amounts of overexpressed Xdsh protein were recovered by the crush method and immunoprecipitation technique. A slight loss in higher molecular weight forms of Xdsh was observed by the crush method, most probably due to a small loss in membranous compartments. This method, however, makes the separation of endogenous Xdsh extracts possible and therefore renders Xdsh proteins in semi-quantitative amounts. Separation of immunoprecipitates or extracts by SDS–PAGE and immunoblotting was followed by antibody incubation. Antiserum to *Drosophila* (anti-Ddsh region I; Yanagawa *et al.*, 1995) or mouse Dsh (anti-Dvl-1; R.Nusse and K.Willert, Stanford University, personal communication) was used to detect either endogenous and ectopic or endogenous Xdsh only, respectively. The anti-mouse Dvl-1/2 antibody, which is directed against a C-terminal portion of the molecule, does not recognize the HA-tagged Xdsh. Anti-HA monoclonal antibody (12CA5, Berkeley Antibody Company), anti-myc monoclonal (Oncogene Science) and anti-myc polyclonal (Santa Cruz Sciences) antibodies were used to detect ectopic Xdsh on Western blots. Secondary antibodies were horseradish peroxidase (HRP)-conjugated goat anti-rat (Amersham), goat anti-mouse (Jackson Laboratories or KPL) or goat anti-rabbit (KPL) antisera. HRP signals were visualized by ECL (Amersham). In consecutive antibody staining of the same blot, HRP activity of the first stain was inactivated in 0.1% sodium azide, washed in Tris-buffered saline (TBS) and restained with a different set of antibodies. Densitometric evaluation of X-ray films was performed using a Gretag D200 densitometer. Inverse log data of a 0.3 × 3 mm area were collected and normalized towards each other to establish relative intensities.

Fluorescence microscopy

Membrane translocation of Xdsh was monitored using an assay previously described (Yang-Snyder *et al*., 1996). mRNAs (40–400 pg) of GFP- or HA-tagged Xdsh or Xdsh deletions were injected or co-injected with 1–2 ng of *frizzled* mRNAs in each blastomere at the 2- to 4-cell stages in animal regions of *Xenopus* embryos. At blastula to early gastrula stages, animal caps were dissected and fixed in 2% paraformaldehyde in phosphate-buffered saline (PBS) for 1 h, rinsed in PBS and directly mounted. Alternatively, they were washed afterwards in TBS/Tween and stained with anti-HA and fluorescein isothiocyanate (FITC)-labeled (Jackson Laboratories) or rhodamine-labeled (Cappel) goat anti-mouse secondary antiserum. Additionally, Texas red–streptavidin (Amersham) sandwich labeling was performed using a biotin-labeled secondary sheep anti-mouse antibody (Amersham). Fluorescence was viewed using a Zeiss Axioplan epifluorescence microscope equipped with a light-intensifying camera (Hamamatsu SIT C4200) and an image processor (Imaging Technology 151) controlled by a VidIm software package (Belford, Stollberg and Fraser, unpublished data) to import images of 16 frames averaged. Adobe Photoshop was used to enhance contrast.

References

Adler,P.N., Krasnow,R.E. and Liu,J. (1997) Tissue polarity points from cells that have higher Frizzled levels towards cells that have lower Frizzled levels. *Curr. Biol.*, **7**, 940–949.

Axelrod,J.D., Matsuno,K., Artavanis-Tsakonas,S. and Perrimon,N. (1996) Interaction between Wingless and Notch signaling pathways mediated by dishevelled. *Science*, **271**, 1826–1832.

Axelrod,J.D., Miller,J.R., Shulman,J.M., Moon,R.T. and Perrimon,N. (1998) Differential recruitment of Dishevelled provides signaling specificity in the planar cell polarity and Wingless signaling pathways. *Genes Dev.*, **12**, 2610–2622.

Bhanot,P., Brink,M., Samos,C.H., Hsieh,J.C., Wang,Y.S., Macke,J.P., Andrew,D., Nathans,J. and Nusse,R. (1996) A new member of the frizzled family from *Drosophila* functions as a wingless receptor. *Nature*, **382**, 225–230.

Bhat,K.M. (1998) frizzled and frizzled 2 play a partially redundant role in wingless signaling and have similar requirements to wingless in neurogenesis. *Cell*, **95**, 1027–1036.

Blitz,I.L. and Cho,K.W. (1995) Anterior neurectoderm is progressively induced during gastrulation: the role of the *Xenopus* homeobox gene *orthodenticle*. *Development*, **121**, 993-1004.

Boutros,M., Paricio,N., Strutt,D.I. and Mlodzik,M. (1998) Dishevelled activates JNK and discriminates between JNK pathways in planar polarity and wingless signaling. *Cell*, **94**, 109–118.

Brannon,M., Gomperts,M., Sumoy,L., Moon,R.T. and Kimelman,D. (1997) A β-catenin/XTcf-3 complex binds to the *siamois* promoter to regulate dorsal axis specification in *Xenopus*. *Genes Dev.*, **11**, 2359–2370.

Cabral,J.H., Petosa,C., Sutcliffe,M.J., Raza,S., Byron,O., Poy,F., Marfatia,S.M., Chishti,A.H. and Liddington,R.C. (1996) Crystal structure of a PDZ domain. *Nature*, **382**, 649–652.

Cadigan,K.M. and Nusse,R. (1997) Wnt signaling: a common theme in animal development. *Genes Dev.*, **11**, 3286–3305.

Cooper,M.T. and Bray,S.J. (1999) Frizzled regulation of Notch signalling polarizes cell fate in the *Drosophila* eye. *Nature*, **397**, 526–530.

Couso,J.P. and Martinez Arias,A. (1994) Notch is required for wingless signaling in the epidermis of *Drosophila*. *Cell*, **79**, 259–272.

Deardorff,M.A., Tan,C., Conrad,L.J. and Klein,P.S. (1998) Frizzled-8 is expressed in the Spemann organizer and plays a role in early morphogenesis. *Development*, **125**, 2687–2700.

Doyle,D.A., Lee,A., Lewis,J., Kim,E., Sheng,M. and MacKinnon,R. (1996) Crystal structures of a complexed and peptide-free membrane protein-binding domain: molecular basis of peptide recognition by PDZ. *Cell*, **85**, 1067–1076.

Fagotto,F., Jho,E., Zeng,L., Kurth,T., Joos,T., Kaufmann,C. and Costantini,F. (1999) Domains of axin involved in protein–protein interactions, wnt pathway inhibition and intracellular localization. *J. Cell Biol.*, **145**, 741–756.

Fanto,M. and Mlodzik,M. (1999) Asymmetric Notch activation specifies photoreceptors R3 and R4 and planar polarity in the *Drosophila* eye. *Nature*, **397**, 523–526.

Gho,M. and Schweisguth,F. (1998) Frizzled signalling controls orientation of asymmetric sense organ precursor cell divisions in *Drosophila*. *Nature*, **393**, 178–181.

Hamada,F. *et al*. (1999) Negative regulation of Wingless signaling by D-axin, a *Drosophila* homolog of axin. *Science*, **283**, 1739–1742.

Hawley,S.H., Wünnenberg-Stapleton,K., Hashimoto,C., Laurent,M.N., Watabe,T., Blumberg,B.W. and Cho,K.W. (1995) Disruption of BMP signals in embryonic *Xenopus* ectoderm leads to direct neural induction. *Genes Dev.*, **9**, 2923–2935.

Heasman,J. (1997) Patterning the *Xenopus* blastula. *Development*, **124**, 4179–4191.

Heslip,T.R., Theisen,H., Walker,H. and Marsh,J.L. (1997) Shaggy and dishevelled exert opposite effects on Wingless and Decapentaplegic expression and on positional identity in imaginal discs. *Development*, **124**, 1069–1078.

Itoh,K., Jacob,J. and Sokol,S.Y. (1998) A role for *Xenopus* Frizzled 8 in dorsal development. *Mech. Dev.*, **74**, 145–157.

Kennedy,M.B. (1995) Origin of PDZ (DHR, GLGF) domains. *Trends Biochem. Sci.*, **20**, 350.

Kennerdell,J.R. and Carthew,R.W. (1998) Use of dsRNA-mediated genetic interference to demonstrate that frizzled and frizzled 2 act in the wingless pathway. *Cell*, **95**, 1017–1026.

Kishida,S., Yamamoto,H., Hino,S., Ikeda,S., Kishida,M. and Kikuchi,A. (1999) DIX domains of Dvl and axin are necessary for protein interactions and their ability to regulate β-catenin stability. *Mol. Cell. Biol.*, **19**, 4414–4422.

Klingensmith,J., Yang,Y., Axelrod,J.D., Beier,D.R., Perrimon,N. and Sussman,D.J. (1996) Conservation of dishevelled structure and function between flies and mice–isolation and characterization of dvl2. *Mech. Dev.*, **58**, 15–26.

Koelle,M.R. and Horvitz,H.R. (1996) EGL-10 regulates G protein signaling in the *C.elegans* nervous system and shares a conserved domain with many mammalian proteins. *Cell*, **84**, 115–125.

Larabell,C.A., Torres,M., Rowning,B.A., Yost,C., Miller,J.R., Wu,M., Kimelman,D. and Moon,R.T. (1997) Establishment of the dorso-ventral axis in *Xenopus* embryos is presaged by early asymmetries in β-catenin that are modulated by the Wnt signaling pathway. *J. Cell Biol.*, **136**, 1123–1136.

Laurent,M.N., Blitz,I.L., Hashimoto,C., Rothbächer,U. and Cho,K.W. (1997) The *Xenopus* homeobox gene *twin* mediates Wnt induction of goosecoid in establishment of Spemann's organizer. *Development*, **124**, 4905–4916.

Lee,J.S., Ishimoto,A. and Yanagawa,S. (1999) Characterization of mouse dishevelled (Dvl) proteins in Wnt/Wingless signaling pathway. *J. Biol. Chem.*, **274**, 21464–21470.

Li,L., Yuan,H., Weaver,C.D., Mao,J., Farr,G.H.,3rd, Sussman,D.J., Jonkers,J., Kimelman,D. and Wu,D. (1999a) Axin and Frat1 interact with dvl and GSK, bridging Dvl to GSK in Wnt-mediated regulation of LEF-1. *EMBO J.*, **18**, 4233–4240.

Li,L., Yuan,H., Xie,W., Mao,J., Caruso,A.M., McMahon,A., Sussman,D.J. and Wu,D. (1999b) Dishevelled proteins lead to two signaling pathways. Regulation of LEF-1 and c-Jun N-terminal kinase in mammalian cells. *J. Biol. Chem.*, **274**, 129–134.

Miller,J.R. and Moon,R.T. (1996) Signal transduction through β-catenin and specification of cell fate during embryogenesis. *Genes Dev.*, **10**, 2527–2539.

Miller,J.R., Rowning,B.A., Larabell,C.A., Yang-Snyder,J.A., Bates,R.L. and Moon,R.T. (1999) Establishment of the dorsal–ventral axis in *Xenopus* embryos coincides with the dorsal enrichment of dishevelled that is dependent on cortical rotation. *J. Cell Biol.*, **146**, 427–437.

Moon,R.T. and Kimelman,D. (1998) From cortical rotation to organizer gene expression: toward a molecular explanation of axis specification in *Xenopus*. *BioEssays*, **20**, 536–545.

Moriguchi,T., Kawachi,K., Kamakura,S., Masuyama,N., Yamanaka,H., Matsumoto,K., Kikuchi,A. and Nishida,E. (1999) Distinct domains of mouse dishevelled are responsible for the c-Jun N-terminal kinase/stress-activated protein kinase activation and the axis formation in vertebrates. *J. Biol. Chem.*, **274**, 30957–30962.

Müller,H., Samanta,R. and Wieschaus,E. (1999) Wingless signaling in the *Drosophila* embryo: zygotic requirements and the role of the frizzled genes. *Development*, **126**, 577–586.

Nasevicius,A., Hyatt,T., Kim,H., Guttman,J., Walsh,E., Sumanas,S., Wang,Y. and Ekker,S.C. (1998) Evidence for a frizzled-mediated wnt pathway required for zebrafish dorsal mesoderm formation. *Development*, **125**, 4283–4292.

Peters,J.M., McKay,R.M., McKay,J.P. and Graff,J.M. (1999) Casein kinase I transduces Wnt signals. *Nature*, **401**, 345–350.

Polakis,P. (1999) The oncogenic activation of β-catenin. *Curr. Opin. Genet. Dev.*, **9**, 15–21.

Ponting,C.P. and Bork,P. (1996) Pleckstrin's repeat performance: a novel domain in G-protein signaling? *Trends Biochem. Sci.*, **21**, 245–246.

Ponting,C.P., Phillips,C., Davies,K.E. and Blake,D.J. (1997) PDZ domains: targeting signalling molecules to sub-membranous sites. *BioEssays*, **19**, 469–479.

Rothbächer,U., Laurent,M.N., Blitz,I.L., Watabe,T., Marsh,J.L. and Cho,K.W.Y. (1995) Functional conservation of the wnt signaling pathway revealed by ectopic expression of *Drosophila* dishevelled in *Xenopus*. *Dev. Biol.*, **170**, 717–721.

Rowning,B.A., Wells,J., Wu,M., Gerhart,J.C., Moon,R.T. and Larabell,C.A. (1997) Microtubule-mediated transport of organelles and localization of β-catenin to the future dorsal side of *Xenopus* eggs. *Proc. Natl Acad. Sci. USA*, **94**, 1224–1229.

Ruel,L., Bourouis,M., Heitzler,P., Pantesco,V. and Simpson,P. (1993) *Drosophila* shaggy kinase and rat glycogen synthase kinase-3 have conserved activities and act downstream of Notch. *Nature*, **362**, 557–560.

Sakanaka,C., Leong,P., Xu,L., Harrison,S.D. and Williams,L.T. (1999) Casein kinase Iε in the Wnt pathway: regulation of β-catenin function. *Proc. Natl Acad. Sci. USA*, **96**, 12548–12552.

Schneider,S., Steinbeisser,H., Warga,R.M. and Hausen,P. (1996) β-catenin translocation into nuclei demarcates the dorsalizing centers in frog and fish embryos. *Mech. Dev.*, **57**, 191–198.

Semenov,M.V. and Snyder,M. (1997) Human dishevelled genes constitute a DHR-containing multigene family. *Genomics*, **42**, 302–310.

Shi,D.L., Goisset,C. and Boucaut,J.C. (1998) Expression of Xfz3, a *Xenopus* frizzled family member, is restricted to the early nervous system. *Mech. Dev.*, **70**, 35–47.

Slusarski,D.C., Corces,V.G. and Moon,R.T. (1997) Interaction of Wnt and a Frizzled homologue triggers G-protein-linked phosphatidylinositol signalling. *Nature*, **390**, 410–413.

Smalley,M.J. *et al*. (1999) Interaction of axin and dvl-2 proteins regulates dvl-2-stimulated TCF-dependent transcription. *EMBO J.*, **18**, 2823–2835.

Sokol,S.Y. (1996) Analysis of Dishevelled signalling pathways during *Xenopus* development. *Curr. Biol.*, **6**, 1456–1467.

Sokol,S.Y., Klingensmith,J., Perrimon,N. and Itoh,K. (1995) Dorsalizing and neuralizing properties of xdsh, a maternally expressed *Xenopus* homolog of dishevelled. *Development*, **121**, 1637–1647.

Strutt,D.I., Weber,U. and Mlodzik,M. (1997) The role of RhoA in tissue polarity and Frizzled signalling. *Nature*, **387**, 292–295.

Sussman,D.J., Klingensmith,J., Salinas,P., Adams,P.S., Nusse,R. and Perrimon,N. (1994) Isolation and characterization of a mouse homolog of the *Drosophila* segment polarity gene *dishevelled*. *Dev. Biol.*, **166**, 73–86.

Theisen,H., Purcell,J., Bennett,M., Kansagara,D., Syed,A. and Marsh,J.L. (1994) *dishevelled* is required during wingless signaling to establish both cell polarity and cell identity. *Development*, **120**, 347–360.

Tsang,M., Lijam,N., Yang,Y., Beier,D.R., Wynshaw-Boris,A. and Sussman,D.J. (1996) Isolation and characterization of mouse dishevelled-3. *Dev. Dynam.*, **207**, 253–262.

Watabe,T., Kim,S., Candia,A., Rothbächer,U., Hashimoto,C., Inoue,K. and Cho,K.W.Y. (1995) Molecular mechanisms of Spemanns organizer formation–conserved growth-factor synergy between *Xenopus* and mouse. *Genes Dev.*, **9**, 3038–3050.

Willert,K., Brink,M., Wodarz,A., Varmus,H. and Nusse,R. (1997) Casein kinase-2 associates with and phosphorylates dishevelled. *EMBO J.*, **16**, 3089–3096.

Wittbrodt,J. and Rosa,F.M. (1994) Disruption of mesoderm and axis formation in fish by ectopic expression of activin variants–the role of maternal activin. *Genes Dev.*, **8**, 1448–1462.

Yanagawa,S., van Leeuwen,F., Wodarz,A., Klingensmith,J. and Nusse,R. (1995) The dishevelled protein is modified by wingless signaling in *Drosophila*. *Genes Dev.*, **9**, 1087–1097.

Yang,Y.S., Lijam,N., Sussman,D.J. and Tsang,M. (1996) Genomic organization of mouse dishevelled genes. *Gene*, **180**, 121–123.

Yang-Snyder,J., Miller,J.R., Brown,J.D., Lai,C.J. and Moon,R.T. (1996) A frizzled homolog functions in a vertebrate wnt signaling pathway. *Curr. Biol.*, **6**, 1302–1306.

Zeng,L. *et al*. (1997) The mouse Fused locus encodes Axin, an inhibitor of the Wnt signaling pathway that regulates embryonic axis formation. *Cell*, **90**, 181–192.